Ecological Engineering 80 (2015) 172–180

Contents lists available at ScienceDirect

Ecological Engineering

journal homepage: www.elsevier.com/locate/ecoleng

Effect of bacteria density and accumulated inert solids on the effluent pollutant concentrations predicted by the constructed wetlands model BIO_PORE

Roger Samsó [a], Jordi Blázquez [a], Núria Agulló [a], Joan Grau [b], Ricardo Torres [b], Joan García [a,*]

[a] GEMMA – Group of Environmental Engineering and Microbiology, Department of Hydraulic, Maritime and Environmental Engineering, Universitat Politècnica de Catalunya-BarcelonaTech, c/ Jordi Girona, 1-3, Building D1, E-08034 Barcelona, Spain
[b] Fluid Mechanics Department, Universitat Politècnica de Catalunya-BarcelonaTech, c/ Urgell 187, E-08036 Barcelona, Spain

ARTICLE INFO

Article history:
Received 3 February 2014
Received in revised form 4 July 2014
Accepted 11 September 2014
Available online 23 October 2014

Keywords:
Local sensitivity
Mesh optimization
Bacteria
Growth
Parallel computing
Batch

ABSTRACT

Constructed wetlands are a widely adopted technology for the treatment of wastewater in small communities. The understanding of their internal functioning has increased at an unprecedented pace over recent years, in part thanks to the use of mathematical models. BIO_PORE model is one of the most recent models developed for constructed wetlands. This model was built in the COMSOL Multiphysics™ software and implements the biokinetic expressions of Constructed Wetlands Model 1 (CWM1) to describe the fate and transport of organic matter, nitrogen and sulphur in horizontal subsurface-flow constructed wetlands. In previous studies, CWM1 was extended with the inclusion of two empirical parameters (M_{bio_max} and M_{cap}) that proved to be essential to provide realistic bacteria growth rates and dynamics. The aim of the current work was to determine the effect of these two parameters on the effluent pollutant concentrations predicted by the model. To that end, nine simulations, each with a different M_{bio_max}-M_{cap} pair, were launched on a high-end multi-processor computer and the effluent COD and ammonia nitrogen concentrations obtained on each simulation were qualitatively compared among them. Prior to this study, a finite element mesh optimization procedure was carried out to reduce computational cost. Results of the mesh optimization procedure indicated that among the 5 tested meshes of different element size, the mesh utilized for this model in previous studies represented a fair compromise between output accuracy and computation time. Results of the sensitivity analysis showed that the value of M_{cap} has a dramatic effect on the simulated effluent concentrations of COD and ammonia nitrogen, which clearly decreased for increasing values of this parameter. On the other hand, the model output was also sensitive to the values of M_{bio_max}, but its effects were less important and no clear relation could be established between its value and the simulated effluent concentration of COD and ammonia nitrogen.

1. Introduction

Constructed wetlands (CWs) are wastewater treatment systems usually applied for communities of less than 2000PE. This technology provides comparable treatment efficiencies with significantly lower energy and maintenance requirements than conventional technologies (García et al., 2010; Puigagut et al., 2007).

However, and due to the diversity and complexity of the physic-chemical and biological processes occurring within CWs, their functioning is far less well understood than that of activated sludge systems. To bridge this knowledge gap, several mathematical models have been developed in recent years to simulate CWs functioning (Meyer et al., 2014; Samsó et al., 2014).

The BIO_PORE model is one of such models and was developed in COMSOL Multiphysics, a commercial finite elements (FE) simulation platform (Meyer et al., 2014; Samsó et al., 2014; Samsó and García, 2013a,b, 2014). This model aims at describing the hydraulics and hydrodynamics of CWs, as well as the removal of the most common pollutants found in wastewater. To that end, it implements the biokinetic model Constructed Wetlands Model 1 (CWM1) (Langergraber et al., 2009), which describes the fate of organic matter, nitrogen and sulphur. This biokinetic model is based on the formulation of the well-known Activated Sludge Model series (ASMs) for aerobic and anoxic processes (Henze et al.,

* Corresponding author. Tel.: +34 93 401 6464; fax: +34 93 401 7357.
E-mail address: joan.garcia@upc.edu (J. García).

http://dx.doi.org/10.1016/j.ecoleng.2014.09.069
0925-8574/

2000) and on the Anaerobic Digestion Model 1 (ADM1) to describe anaerobic processes (Batstone et al., 2002).

In BIO_PORE two logistic functions are added to the original formulation of CWM1, which involve two new empirical parameters: M_{bio_max} and M_{cap} (Samsó and García, 2013a). These two parameters represent, respectively, the maximum microbial biomass (carrying capacity) and the maximum amount of particulate solids that can be maintained in a representative volume of granular material. The function involving M_{bio_max} has already been used in several bioclogging studies (Brovelli et al., 2009) and adds a negative feedback term to the growth of all bacteria groups to prevent their unlimited growth in areas where substrates concentrations are high. On the other hand, the expression involving parameter M_{cap} also adds a negative feedback term to the growth equations, but in this case it decreases the growth rate of bacteria due to the progressive accumulation of inert solids in the pore space of the granular media (Samsó and García, 2014). Our previous studies proved the importance of these two functions in order to obtain realistic bacteria concentrations within the granular media (Samsó and García, 2013a, 2014). As bacterial communities play a major role on the treatment of wastewater in CWs, these two functions also improved the model predictions regarding effluent pollutant concentrations.

However, in these previous studies, although a discussion was made around the impact of parameters M_{bio_max} and M_{cap} on the concentration of solids and the different bacterial groups within the bed, their impact on the effluent pollutant concentrations was not evaluated.

In this study we carried out a sensitivity analysis to identify the individual contributions of the two uncertain input model parameters (i.e., M_{bio_max} and M_{cap}) to the output uncertainty (i.e., effluent pollutant concentrations of COD and ammonia and ammonium nitrogen)(Sin et al., 2009).

Sensitivity analysis methods are generally classified between qualitative and quantitative methods and between local and global techniques, and the choice of the method is generally driven by computational cost (Cariboni et al., 2007).

Most of the sensitivity analysis studies carried out in the field of wastewater treatment modelling are of local nature and use a differential analysis of outputs with respect to parameters (Sin et al., 2011). Local methods, are the simplest ones to sensitivity analysis, and consist on repeatedly varying one parameter at a time (OAT) while holding the others fixed (Hamby, 1994).

These sort of methods, which are employed in the current work, are economical from a computational point of view, but they provide qualitative sensitivity measures (they rank the input factors in order of importance, but do not quantify how much a given factor is more important than another) (Dimov and Georgieva, 2010).

To perform the sensitivity analysis, the BIO_PORE model was used with the same domain, parameter values and initial and boundary conditions than in our previous paper in which the model was calibrated (Samsó and García, 2013a). Due to the large computational cost associated with solving the model for a simulated period of an entire year of operation of a wetland (up to 16 h for dense FE meshes with a current desktop computer), and due to the large number of simulations needed for the current and for further studies, a previous mesh optimization procedure was carried out. The objective of this part of the study was to find the FE mesh which would provide the best compromise between numerical solutions accuracy (lower discretization error) and computational cost.

The two empirical parameters discussed in this work are essential to obtain realistic bacteria concentrations when simulating CWs and this study shows how they affect the effluent pollutant concentrations predicted by the BIO_PORE model. In this work we also exploited the batch and parallel computation functionalities of COMSOL Multiphysics™ on a high-end multi-processor computer which is easily justified by the large number of simulations performed.

Table 1
Description of the components considered in BIO_PORE model. S_i are dissolved species (all in the aqueous phase by definition) and X_i are particulate species (either in aqueous or solid phase).

Componenet	Description	Unit	Phase
S_O	Dissolved oxygen	mg COD $\cdot L^{-1}$	Aqueous
S_F	Soluble fermentable COD	mg COD $\cdot L^{-1}$	Aqueous
S_A	Fermentation products as acetate as COD	mg COD $\cdot L^{-1}$	Aqueous
S_I	Inert soluble COD	mg COD $\cdot L^{-1}$	Aqueous
X_{Sm}	Aqueous slowly biodegradable particulate COD	mg COD $\cdot L^{-1}$	Aqueous
X_{Sf}	Solid slowly biodegradable particulate COD	mg COD $\cdot L^{-1}$	Solid
X_{Im}	Aqueous inert particulate COD	mg COD $\cdot L^{-1}$	Aqueous
X_{If}	Solid inert particulate COD	mg COD $\cdot L^{-1}$	Solid
S_{NO}	Nitrite and nitrate nitrogen	mg N $\cdot L^{-1}$	Aqueous
S_{NH}	Ammonium and ammonia nitrogen	mg N $\cdot L^{-1}$	Aqueous
S_{SO4}	Sulphate sulphur	mg S $\cdot L^{-1}$	Aqueous
S_{H2S}	Dihydrogensulphide sulphur	mg S $\cdot L^{-1}$	Aqueous

2. Methods

The local parameter sensitivity analysis and the mesh optimization procedure were performed using the exact same domain, parameter values and boundary and initial conditions as in Samsó and García (2013a). For this reason, only the basic equations of the BIO_PORE model are described in this section. For an in-depth description of all model equations the reader is referred to the original source. All simulations performed in this study were run for the entire first year of operation of a pilot wetland.

2.1. BIO _PORE model description

2.1.1. Governing equations

In BIO_PORE model, the saturated porous media flow is described using the Darcy equation (Eq. (1)).

$$q_i = -K_{ij}\frac{\partial H}{\partial x_j} \tag{1}$$

where, q_i is the specific discharge $[LT^{-1}]$, K_{ij} is the saturated hydraulic conductivity tensor $[LT^{-1}]$, and $(\partial H/\partial x_j)$ the hydraulic gradient vector (unitless). Since in CWs both saturated and unsaturated conditions coexist, the *Deformed Geometry* node of COMSOL Multiphysics™ was used to dynamically adjust the top boundary of the model domain to the simulated shape and location of the water table.

The fate and transport of the aqueous phase (mobile) wastewater components of CWM1 (Table 1) are described with reactive transport equations, one for each component, in which the reactive term accounts for the production/consumption of the substrate through microbial activity (Eq. (2))(Clement et al., 1998).

$$\frac{\partial C_k}{\partial t} = \frac{\partial}{\partial x_i}\left(D_{ij}\frac{\partial C_k}{\partial x_j}\right) - \frac{\partial}{\partial x_i}(q_i C_k) + r_r - r_{att} + r_{\det} + s_s \tag{2}$$

where $k = 1, 2 \ldots m$ and m is the total number of aqueous phase species (dissolved and particulate, see Table 1). C_k $[ML^{-3}]$ is the concentration of the kth aqueous phase species, D_{ij} $[L^2T^{-1}]$ is the

Table 2
Functional bacterial groups considered in BIO_PORE. Bacteria concentrations are given in units of COD (mg COD ·L^{-1}).

Component	Description	Phase
X_H	Heterotrophic bacteria	Solid
X_A	Autotrophic nitrifying bacteria	Solid
X_{FB}	Fermenting bacteria	Solid
X_{AMB}	Acetotrophic methanogenic bacteria	Solid
X_{ASRB}	Acetotrophic sulphate reducing bacteria	Solid
X_{SOB}	Sulphide oxidizing bacteria	Solid

hydrodynamic dispersion tensor. q_i $[LT^{-1}]$ is the specific discharge and acts as the coupling variable between Eqs. (1) and (2). r_r $[ML^{-3}T^{-1}]$ is the reaction rate of the kth species in the aqueous phase. r_{att} $[ML^{-3}T^{-1}]$ and r_{det} $[ML^{-3}T^{-1}]$ are attachment and detachment rates, respectively, and are used to simulate mass exchanges between the aqueous and the solid phases of particulate components X_S and X_I. s_s $[ML^{-3}T^{-1}]$ is the source/sink term, which represents external sources or sinks of species C_k. This last term is only used to simulate oxygen release and nutrients uptake through plant roots (see Samsó and García, 2013a for more details).

On the other hand, Eq. (3) describes the fate of the solid phase (immobile) species (Table 1):

$$\frac{d\check{C}_l}{dt} = \check{r}_r + r_{att} - r_{\det} \tag{3}$$

where $l = 1, 2, \ldots n$ and n is the total number of solid phase species (particulate only). $\check{C}_l[ML^{-3}]$ is the concentration of the lth species and $\check{r}_r[ML^{-3}T^{-1}]$ is the reaction rate of the lth species on the solid phase.

The growth and decay rates of each bacteria group considered in CWM1 (Table 2) are described using Monod expressions (Monod, 1949), to which the product of two logistic expressions was added (Eq. (4)):

$$f_{GL} = \left(1 - \frac{M_{bio}}{M_{bio\_\max}}\right)\left(1 - \frac{M_{X_{If}}}{M_{cap}}\right) \tag{4}$$

where, M_{bio_max} and M_{cap} $[M]$ are two empirical parameters representing, respectively, the maximum microbial biomass (carrying capacity) and the maximum amount of particulate solids that can be maintained in a representative volume of granular material. On the other hand, M_{bio} and $M_{X_{If}}$ $[M]$ are, respectively, the sum of the total microbial biomass and the actual mass of immobile X_I present in the representative volume.

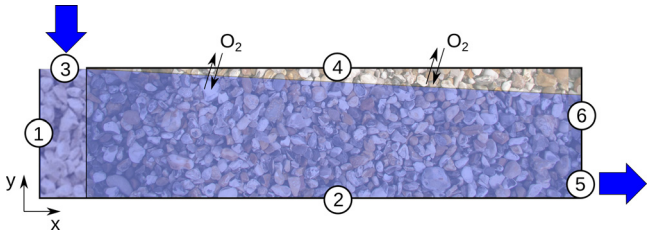

Fig. 1. Model domain, representing a longitudinal section of wetland *C2* in García et al. (2004a), and numbers of the different boundaries (obtained from Samsó and García (2013a)). The numbers identify the different boundaries of the domain. Numbers 3 and 5 correspond to the inlet and outlet sections, respectively.

Table 3 shows the biokinetic processes rates of the BIO_PORE model resulting from the inclusion of Eq. (4) to the original formulation of CWM1.

Notice that all kinetic parameters of CWM1 are interpolated to account for water temperature variations.

2.1.2. Model domain

The model domain corresponds to a longitudinal section of wetland *C2* of the pilot system described in García et al. (2004a,b) (Fig. 1). This wetland was 10.3 m long and 5.3 m wide, with a bottom slope of 1%. The granular media consisted of fine granitic gravel (D_{60} = 3.5 mm, C_u = 1.7, initial porosity n = 40%) with a depth of approximately 0.6 m at the inlet and 0.7 m at the outlet.

2.1.3. Initial and boundary conditions

Experimentally measured flow-rates, ranging from 1.1 to 2.45 m^{3}d^{-1} were imposed at boundary 3 (inlet) and a hydraulic head of 0.5 m at boundary 5 (outlet). An hydraulic head of 0.5 m was set as the initial condition for the Darcy equation.

For the transport equations, inflow concentrations of the components listed in Table 1, which were obtained from field measurements (see Section 2.1.4), were imposed at boundary 3. An outflow boundary condition was imposed at boundary 5. The initial concentrations of all substrates within the wetland were set to 10 mg L^{-1}.

Table 3
Processes rates in mg ·d^{-1} (adapted from Langergraber et al., 2009).

j	Process	Process rate ρ_j
1	Hydrolysis X_{Sf}	$k_h \left[\frac{\frac{X_{Sf}}{X_H+X_{FB}}}{K_X\left(\frac{X_{Sf}}{X_H+X_{FB}}\right)}\right](X_H + \eta_h X_{FB})$
2	Aerobic growth of X_H on S_F	$\mu_H \cdot f_{GL}\left(\frac{S_F}{K_{SFH}+S_F}\right)\left(\frac{S_F}{S_F+S_A}\right)\left(\frac{S_O}{K_{SOH}+S_O}\right)\left(\frac{S_{NH}}{K_{SNHH}+S_{NH}}\right)\left(\frac{K_{SH2SH}}{K_{SH2SH}+S_{H2S}}\right)X_H$
3	Anoxic growth of X_H on S_F	$\eta_g \cdot \mu_H \cdot f_{GL}\left(\frac{S_F}{K_{SFH}+S_F}\right)\left(\frac{S_F}{S_F+S_A}\right)\left(\frac{K_{SOH}}{K_{SOH}+S_O}\right)\left(\frac{S_{NO}}{K_{SNOH}+S_{NO}}\right)\left(\frac{S_{NH}}{K_{SNHH}+S_{NH}}\right)\left(\frac{K_{SH2SH}}{K_{SH2SH}+S_{H2S}}\right)X_H$
4	Aerobic growth of X_H on S_A	$\mu_H \cdot f_{GL}\left(\frac{S_A}{K_{SAH}+S_A}\right)\left(\frac{S_A}{S_F+S_A}\right)\left(\frac{S_O}{K_{SOH}+S_O}\right)\left(\frac{S_{NH}}{K_{SNHH}+S_{NH}}\right)\left(\frac{K_{SH2SH}}{K_{SH2SH}+S_{H2S}}\right)X_H$
5	Anoxic growth of X_H on S_A	$\eta_g \mu_H \cdot f_{GL}\left(\frac{S_A}{K_{SAH}+S_A}\right)\left(\frac{S_A}{S_F+S_A}\right)\left(\frac{K_{SOH}}{K_{SOH}+S_O}\right)\left(\frac{S_{NO}}{K_{SNOH}+S_{NO}}\right)\left(\frac{S_{NH}}{K_{SNHH}+S_{NH}}\right)\left(\frac{K_{SH2SH}}{K_{SH2SH}+S_{H2S}}\right)X_H$
6	Lysis of X_H	$b_X X_H$
7	Aerobic growth of X_A on S_{NH}	$\mu_A \cdot f_{GL}\left(\frac{S_{NH}}{K_{SNHA}+S_{NH}}\right)\left(\frac{S_O}{K_{SOA}+S_O}\right)\left(\frac{K_{SH2SA}}{K_{SH2SA}+S_{H2S}}\right)X_A$
8	Lysis of X_A	$b_A X_A$
9	Growth of X_{FB}	$\mu_{FB} \cdot f_{GL}\left(\frac{S_F}{K_{SFFB}+S_F}\right)\left(\frac{K_{SH2SFB}}{K_{SH2SFB}+S_{H2S}}\right)\left(\frac{K_{SOFB}}{K_{SOFB}+S_O}\right)\left(\frac{K_{SNOFB}}{K_{SNOFB}+S_{NO}}\right)\left(\frac{S_{NH}}{K_{SNHFB}+S_{NH}}\right)X_{FB}$
10	Lysis of X_{FB}	$b_{FB} X_{FB}$
11	Growth of X_{AMB}	$\mu_{AMB} \cdot f_{GL}\left(\frac{S_A}{K_{SAMB}+S_A}\right)\left(\frac{K_{SH2SAMB}}{K_{SH2SAMB}+S_{H2S}}\right)\left(\frac{K_{SOAMB}}{K_{SOAMB}+S_O}\right)\left(\frac{K_{SNOAMB}}{K_{SNOAMB}+S_{NO}}\right)\left(\frac{S_{NH}}{K_{SNHAMB}+S_{NH}}\right)X_{AMB}$
12	Lysis of X_{AMB}	$b_{AMB} X_{AMB}$
13	Growth of X_{ASRB}	$\mu_{ASRB} \cdot f_{GL}\left(\frac{SA}{K_{SAASRB}+S_A}\right)\left(\frac{S_{SO4}}{K_{SO4ASRB}+S_{SO4}}\right)\left(\frac{K_{SH2SASRB}}{K_{SH2SASRB}+S_{H2S}}\right)\left(\frac{K_{SOASRB}}{K_{SOASRB}+S_O}\right)\left(\frac{K_{SNOASRB}}{K_{SNOASRB}+S_{NO}}\right)\left(\frac{S_{NH}}{K_{SNHASRB}+S_{NH}}\right)X_{ASRB}$
14	Lysis of X_{XASRB}	$b_{ASRB} X_{ASRB}$
15	Aerobic growth of X_{SOB} on S_{H2S}	$\mu_{SOB} \cdot f_{GL}\left(\frac{S_{H2S}}{K_{SH2SSOB}+S_{H2S}}\right)\left(\frac{S_O}{K_{SOSOB}+S_O}\right)\left(\frac{S_{NH}}{K_{SNHSOB}+S_{NH}}\right)X_{SOB}$
16	Anoxic growth of X_{SOB} on S_{H2S}	$\mu_{SOB} \cdot f_{GL} \cdot \eta_{SOB}\left(\frac{S_{H2S}}{K_{SH2SSOB}+S_{H2S}}\right)\left(\frac{S_{NO}}{K_{SNOSOB}+S_{NO}}\right)\left(\frac{K_{SOSOB}}{K_{SOSOB}+S_O}\right)\left(\frac{S_{NH}}{K_{SNHSOB}+S_{NH}}\right)X_{SOB}$
17	Lysis of X_{SOB}	$b_{SOB} X_{SOB}$

Table 4
Values of the hydraulic and hydrodynamic parameters of the granular media.

Parameter	Description	Unit	Value
α_L	Longitudinal dispersivity	m	0.05
α_T	Transverse dispersivity	m	0.005
K	Hydraulic conductivity	m d^{-1}	50

The initial concentrations of the different bacteria groups within the wetland were set to 1 mg L^{-1} to recreate start-up conditions.

2.1.4. Experimental data and parameter values

The experimental data measured along the first year of operation of the pilot wetland and used to feed the model consisted of: 39 values of flow rate, 32 values of water temperature, 31 values of inflow COD and 33 values of inflow $NH_4 - N$. The fractioning of the inflow COD was made using recommended values for primary effluents in ASMs (Henze et al., 2000): 15% S_F, 50% X_{Sm} (0% X_{Sf}), 20% S_A, 5% S_I and 10% X_{Im} (0% X_{If}). 28 values of COD and 34 of $NH_4 - N$ were measured at the outlet of the pilot wetland during the same period of time.

The inflow concentrations of the rest of components of CWM1 (0 mg L^{-1} for S_{NO} and S_{H2S}, and 72 mg L^{-1} for S_{SO4}) correspond to mean values measured from different samples extracted from the same pilot wetland by García et al. (2004b). Inflow oxygen concentration was set to zero, since *DO* concentration in primary treated wastewater is usually very small (Tyroller et al., 2010).

Values of the hydraulic and hydrodynamic parameters obtained by Samsó and García (2013a) and utilized for all simulations are shown in Table 4.

2.2. Mesh optimization

After a previous detailed study with simplified versions of the model (progressively increasing the number of functional bacterial groups)(results not shown), 5 triangular meshes of different elements densities (Table 5) were chosen to perform the mesh optimization of the complete model (with all bacteria groups listed in Table 2). Among those meshes, $M_{0.1}$ was the coarsest, $M_{0.025}$ the most dense and $M_{BIO-PORE}$ was the one used by Samsó and García (2013a,b). $M_{BIO-PORE}$ was the only mesh with a predefined number of elements at boundaries 3 (20 elements), 4 (550 elements) and 5 (7 elements), which were reckoned as the most critical ones numerically (large concentration gradients).

Simulated effluent concentrations of COD (sum of S_F, S_A, S_I, X_{Sm} and X_{Im}) and S_{NH}, as well as the simulation time were recorded for all different meshes. The Sum of squared errors (SSE) for the effluent COD and S_{NH} curves for all different meshes were calculated using the finer mesh ($M_{0.025}$) as a reference, to showcase the progressive accuracy gains with increasing mesh densities. Following this approach, the optimal mesh corresponds to that after which any further increments on the number of elements do not produce notable improvements on the numerical accuracy (lower discretization error) of the solution (SSE remains fairly constant). Moreover, for evident practical reasons, the optimal mesh is also that with the shortest computational cost/time.

Table 5
Meshes used in the mesh optimization procedure.

Mesh	Maximum element size (m)	Number of elements
$M_{0.1}$	0.1	1860
$M_{0.04}$	0.04	11446
$M_{BIO-PORE}$	0.05[a]	19851
$M_{0.03}$	0.03	20064
$M_{0.025}$	0.025	28884

[a] Note that $M_{BIO-PORE}$ was built with a maximum element size of 0.05 m but fixing the number of elements at boundaries 3 (20 elements), 4 (550 elements) and 5 (7 elements), and its total number of elements is very similar to that of $M_{0.03}$.

Table 6
Combinations of M_{cap} and M_{bio_max} values for the different simulations carried out for the local sensitivity analysis.

Simulation	M_cap (kg VS m^{-3})	M_bio_max (kg VS m^{-3})
$S_{15-0.5}$	15	0.5
$S_{15-0.3}$	15	0.3
$S_{15-0.1}$	15	0.1
$S_{10-0.5}$	10	0.5
$S_{10-0.3}$	10	0.3
$S_{10-0.1}$	10	0.1
$S_{5-0.5}$	5	0.5
$S_{5-0.3}$	5	0.3
$S_{5-0.1}$	5	0.1

2.3. Parameter sensitivity

The sensitivity of the model output to the values of M_{bio_max} and M_{cap} was studied by giving three different values to each of the two parameters and running a different simulation for each different pair (9 simulations in total) (Table 6). The reasons for selecting the values of Table 6 are discussed later in the text. Notice that the range of variability of M_{cap} was smaller than that of M_{bio_max}. In the first case, the highest value of M_{cap} was 3 times the lowest, whereas for M_{bio_max} the highest was 5 times the lowest.

The sensitivity of the two parameters was determined qualitatively by comparing the effluent concentrations of COD among them with the 9 different parameter pairs. The same was done for the simulated effluent concentrations of S_{NH}. A qualitative comparison was made between the effluent concentrations of COD and S_{NH} obtained with each parameter pair.

The mesh used to execute all these processes was the optimum mesh obtained in the previous step (Section 2.2).

2.4. Launching simulations and hardware specifications

In this work two different computers were used. For the mesh optimization procedure, a desktop PC was used. This computer features an Intel Xenon E5-1620 processor with 4 cores (8 threads) running at a frequency of 3600 GHz and 16 GB of RAM memory. The Linux kernel and COMSOL Multiphysics™ versions installed on this computer were 3.2.0-56 and v4.3b, respectively.

On the other hand, for the sensitivity analysis the cluster functionalities of COMSOL Multiphysics were used to run several simulations in parallel on a high-end multi-processor computer. This computer consisted of 4 CPUs *AMD Opteron 6140* with 8 cores each (2.6 GHz), a total of 64 GB of RAM memory and run Linux Kernel 2.6.38. The COMSOl Multiphysics™ version installed in this machine was v4.2a. Since this machine was shared with other researchers, only 3 parallel simulations (using 4 CPU cores each) were launched at a time (see Fig. 2). Therefore only 12 cores, out of the 32 available, were utilized. A bash script was used to automatically launch each different batch of 3 parallel simulations without any intervention.

3. Results and discussion

3.1. Mesh optimization

In the current study the focus was not on how well or bad simulated effluent concentrations fit experimental data, since that discussion was already made in Samsó and García (2013a), but

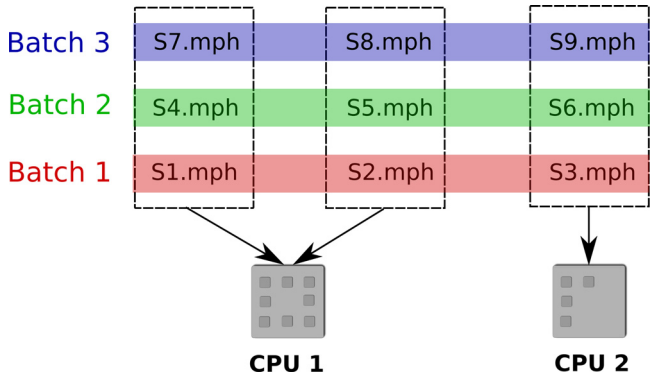

Fig. 2. CPU and processor utilization in the high-end multi-processor computer during the sensitivity analysis. Model files built in COMSOL Multiphysics™ have *mph* extension. Three batches of 3 parallel simulations, each with a different $M_{cap} - M_{bio,max}$ pair (see Table 6), were launched. Each simulation took up only 4 processor cores. All cores of CPU1 were used, while CPU2 was only loaded to a 50%.

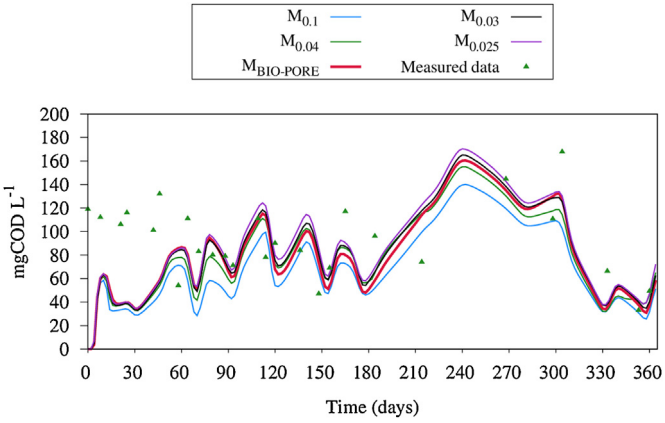

Fig. 3. Simulated effluent COD concentrations obtained from the mesh optimization procedure with the meshes of Table 5.

rather on the comparison of the simulation results obtained with different meshes. However, note that the poor fitting of the simulated effluent COD and S_{NH} with experimental data at the beginning of all simulations (Figs. 3 and 4), was due to the fact that initial bacteria and accumulated solids concentrations were underestimated. However, after around 70 days of simulated time, the fitting improved.

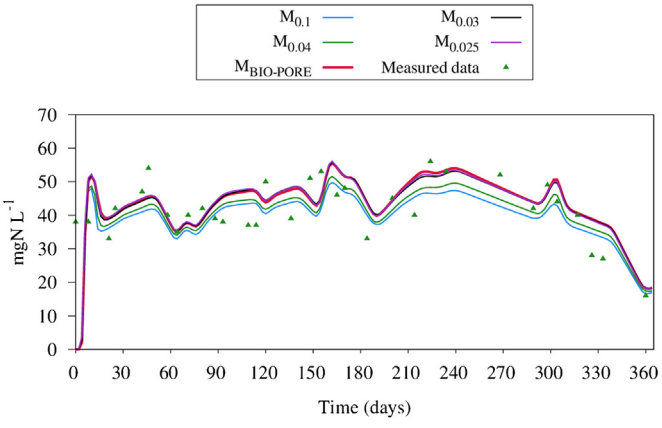

Fig. 4. Simulated effluent S_{NH} concentrations obtained from the mesh optimization procedure with the meshes of Table 5.

Table 7
Number of elements and simulation time for each of the meshes used for mesh optimization.

Mesh	Number of triangular elements	Simulation time (hours)
$M_{0.1}$	1860	1.04
$M_{0.04}$	11446	5.41
$M_{BIO-PORE}$	19851	9.96[a]
$M_{0.03}$	20064	9.53
$M_{0.025}$	28884	16.30

[a] Notice that although $M_{BIO-PORE}$ had fewer elements than $M_{0.03}$ its simulation time was slightly higher. Notice as well that $M_{BIO-PORE}$ was the only one of the selected meshes with higher elements density in boundaries 3, 4 and 5 (see Fig. 1).

Note that for the mesh optimization procedure we did not quantify the discretization error, but rather we qualitatively evaluated the accuracy gains obtained by increasing mesh densities. There are several works in literature dealing with the quantification of the discretization error, and the most popular approach is the Richardson extrapolation (Roache, 1994; Roy, 2005). However, this method imposes strict conditions on the type and properties of the meshes to be used (e.g., uniform meshes). In our study, we used non-uniform meshes as well as the deformed geometry node of COMSOL Multiphysics™, which modifies the shape of the mesh and the location of the nodes over time, and according to the location of the water table. Therefore the quantification of the error was discarded because the imposed restrictions could not be fulfilled.

Figs. 3 and 4 show that the effluent pollutant concentrations of COD and S_{NH} obtained with the different meshes (Table 5) are visually different in some cases.

Finer FE meshes provide more accurate numerical results. Thus in our study, mesh $M_{0.025}$, with a maximum element size of 2.5 cm and a total number of 28,884 elements is the one giving more accurate results. Despite even better results could have been obtained by further refining the mesh, the total simulation time of $M_{0.025}$ (16 h and 18 min) was already seen as too large for practical reasons. Moreover, refining the mesh to such an extent would only make sense if field data, which is given as model input and later used to compare with simulated effluent concentrations, had been gathered in higher frequency. In fact, Fig. 4 clearly shows that almost identical results were obtained for simulated effluent S_{NH} concentrations with meshes $M_{BIO-PORE}$ and $M_{0.03}$ which account for c.a. 30% less elements than $M_{0.025}$. That is also confirmed with the tendency of the SSE for S_{NH} (Fig. 6), which shows clear signs of stabilization already with meshes $M_{BIO-PORE}$ and $M_{0.03}$. Therefore, further mesh refinements would not improve the description of the effluent S_{NH} concentrations. In the case of COD (Fig. 3), although the differences between the curves obtained with different meshes were higher than for S_{NH}, and the SSE was not as stable either (Fig. 5), the maximum difference of effluent COD concentrations obtained with meshes $M_{BIO-PORE}$ and $M_{0.025}$ was lower than 15 mg COD $\cdot L^{-1}$, which was only around 8% the maximum effluent COD concentration simulated with mesh $M_{0.025}$.

Table 7 shows that, in general, the simulation time increased with increasing mesh densities. $M_{BIO-PORE}$ was the exception, and although it had 213 less elements than $M_{0.03}$ the former took 25 min more than the later to reach the final solution (see Table 7). The most likely reason for that is that the mesh element quality of $M_{BIO-PORE}$ was lower than that of $M_{0.03}$ and thus the solver algorithm required a few more iterations at every time step to reach a solution. In fact, $M_{BIO-PORE}$ was the one with the second largest maximum element size (0.05 cm), only after $M_{0.1}$, but in contrast it was the mesh with the highest elements densities in boundaries 3, 4 and 5, which were the ones accounting for the highest concentration gradients. The relation between number of elements and simulated time can also be observed in Figs. 5 and 6, and shows that a linear relationship ($R^2 = 0.97$) exists between the two.

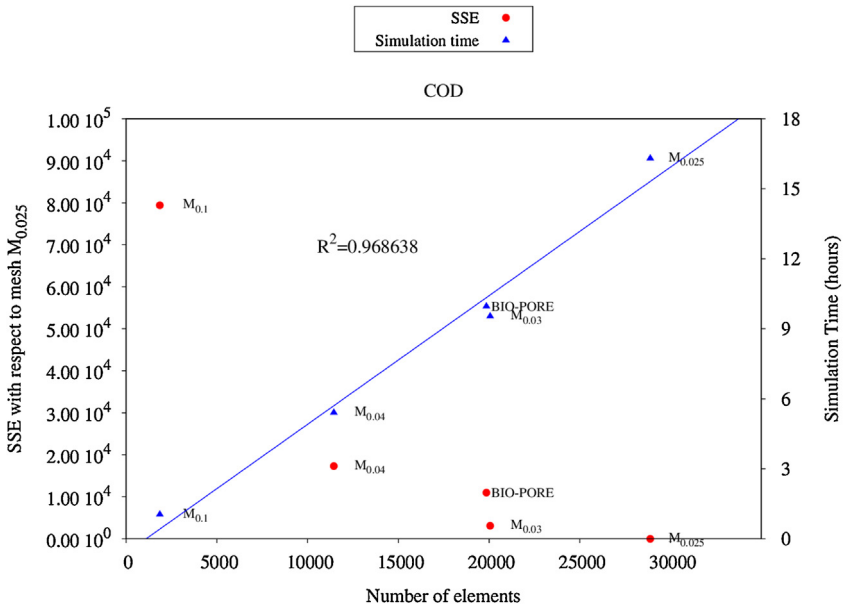

Fig. 5. Sum of squared errors (SSE) with respect to $M_{0.025}$ (left *y*-axis) and simulation time (right *y*-axis) for the simulated effluent COD concentrations obtained with meshes of different elements density (see Table 5). The blue line shows the positive linear relationship (R^2 = 0.97) between the number of triangular elements of the mesh and the simulation time. (For interpretation of the references to color in this figure legend, the reader is referred to the web version of this article.)

According to these results, the mesh with a better compromise between numerical accuracy and simulation time was $M_{0.03}$. The results obtained with mesh $M_{BIO-PORE}$ were almost as good as those obtained with $M_{0.03}$ (see Figs. 3–6), and since mesh $M_{BIO-PORE}$ had already been used successfully in a previous work (Samsó and García, 2013a), it was chosen as the one to be used for the sensitivity analysis.

3.2. Parameter sensitivity

Despite BIO_PORE includes more than 50 parameters, only the sensitivity of M_{bio_max} and M_{cap} was analysed because they are two new additions to the formulation of CWM1. Moreover, the sensitivity of the different parameters of CWM1 has already been studied in other works (Mburu et al., 2012). Note that the type of analysis carried out in this work is a local sensitivity analysis, which only addresses sensitivity relative to the point estimates chosen and not for the entire parameter distribution (Hamby, 1994).

The first parenthesis of Eq. (4) (involving M_{bio_max}) limits the maximum concentration of bacteria that each pore of the granular media can hold (carrying capacity) by stopping the growth of bacteria once M_{bio} reaches the value of M_{bio_max}. The second parenthesis works in the same way, but M_{cap} corresponds to the maximum

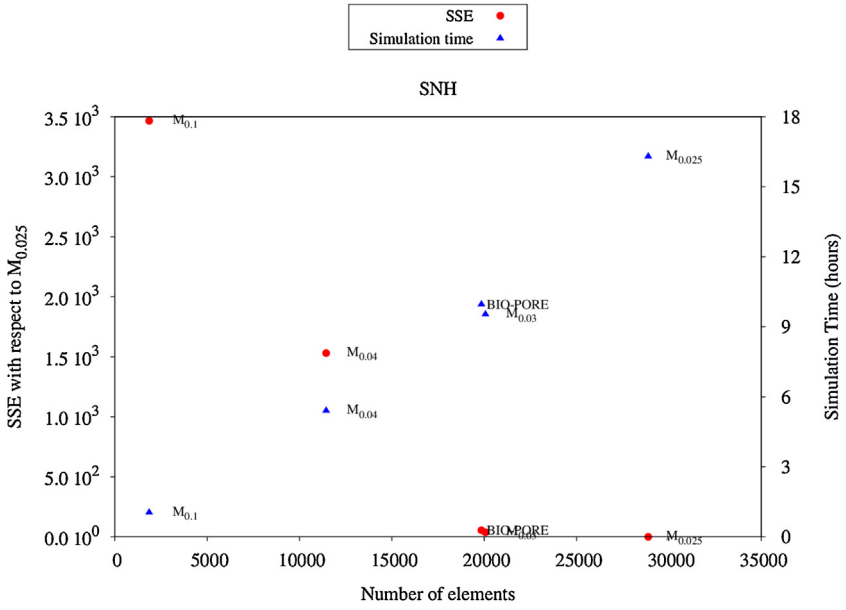

Fig. 6. Sum of squared errors (SSE) with respect to $M_{0.025}$ (left *y*-axis) and simulation time (right *y*-axis) for the simulated effluent S_{NH} concentrations obtained with meshes of different elements density (see Table 5). The R^2 of the linear regression of the simulation time is the same as in Fig. 5, since all data shown in both figures was obtained from the same simulations (each focusing on different model outputs).

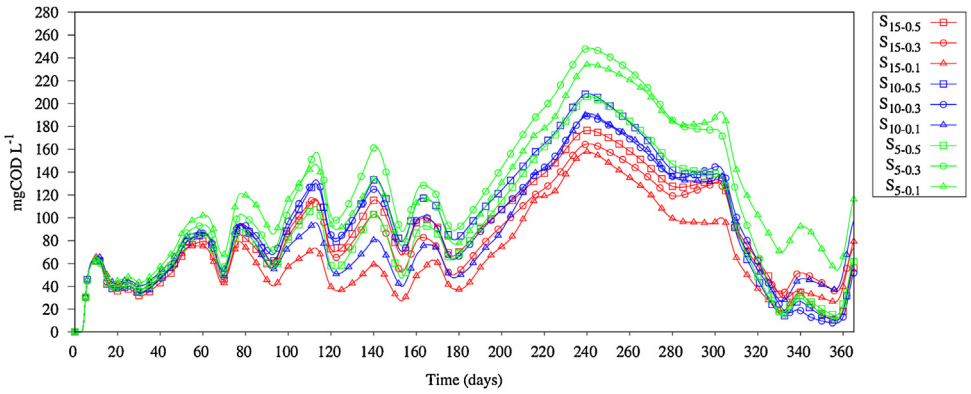

Fig. 7. Effluent COD concentrations obtained with the combinations of M_{bio_max} and M_{cap} shown in Table 6.

amount of particulate solids (X_{Sf} and X_{If}) porosity can hold, and bacterial growth stops once $M_{X_{If}} = M_{cap}$.

The values given to parameters M_{bio_max} were chosen based on our previous experiences with the BIO_PORE model, since no literature values for these parameters exist for CWs. In fact the intermediate value of this parameter used in the current work was that obtained from the calibration of the model in Samsó and García (2013a), and the other two were chosen to be at a sound distance from the first. On the other hand, the amount of accumulated solids in horizontal subsurface flow CWs presents a great variability depending on the COD and TSS loading rates and on the turn-over rates. Measurements carried out by Caselles-Osorio et al. (2007) in 6 full-scale horizontal subsurface flow CWs showed that accumulated solids ranged from as low as 2.3 kg VS $\cdot m^{-2}$ up to 57.3 kg VS $\cdot m^{-2}$ (between around 6 and 162 kg COD $\cdot m^{-3}$, considering an average wetland depth of 0.5 m and that 1 g VS $\approx$1.42 *gCOD* (Samsó and García, 2014)). In this study we selected the values of M_{cap} to be in the lower part of that range, since the gravel size of the pilot system was quite fine (D_{60} = 3.5 mm and C_u = 1.7).

Although the simulated effluent concentrations of the rest of model components could have also been studied, only COD and S_{NH} were used for the sake of brevity and because these are the two most widely used water quality indicators. Total COD also lumps the concentration of several model components (S_F, S_A, S_I, X_{sm}, X_{Im}), which are affected by many different bacterial processes, and will thus be sensitive to changes in bacterial concentrations within the wetland. On the other hand, the effect of these parameters on the bacteria and solids concentrations within the bed was not studied in the current work since this discussion was already made in previous papers (Samsó and García, 2013b, 2014).

Results indicate that simulated concentrations of COD (Fig. 7) and S_{NH} (Fig. 8) were very sensitive to the values of M_{bio_max} and M_{cap}. At the beginning of all simulations, effluent concentrations obtained with the different pairs of M_{bio_max} and M_{cap} were very similar, and it was not until around simulated day 60 that they started diverging. Figs. 7 and 8 show that the parameter with the biggest impact on COD and S_{NH} effluent concentrations was M_{cap}, and the higher its value, and thus the higher the capacity of porosity to retain particulate solids (X_{If} and X_{Sf}), the lower the effluent concentrations of the two pollutants. A possible reasoning for this behaviour is that for high values of M_{cap} the amount of slowly biodegradable particulate COD (X_{Sf}) that can be reached in the granular media is much higher than that the maximum bacteria biomass present in the same location (which is limited by the value of M_{bio_max}) can biodegrade, and so they accumulate. Therefore this accumulated organic matter, which also contains a fraction of organic nitrogen, is retained within the system and does not add to the concentrations of COD and S_{NH} measured at the outlet.

On the other hand, although perturbations of the M_{bio_max} value produced observable changes in the effluent COD and S_{NH} concentrations, these changes were smaller than those produced by changing the value of M_{cap}. Regarding the effluent COD concentrations (Fig. 7), for M_{cap} = 15 kgVS$\cdot m^{-3}$ and M_{cap} = 10 kgVS$\cdot m^{-3}$, the higher the value of M_{bio_max} the higher the effluent

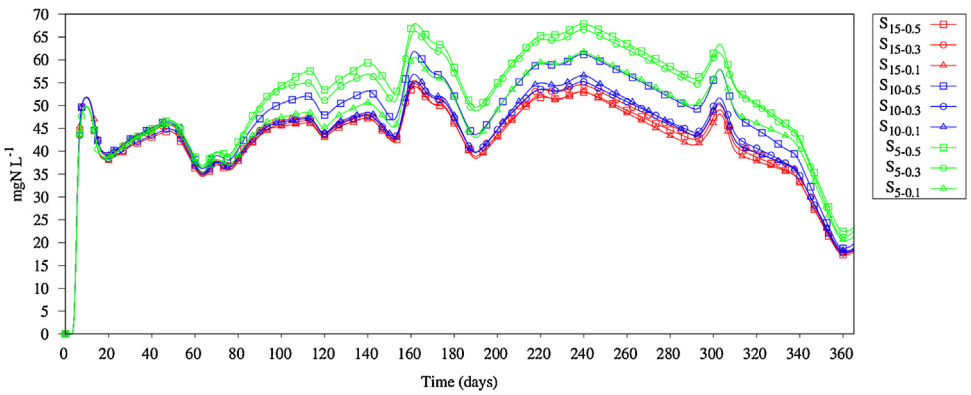

Fig. 8. Effluent S_{NH} concentrations obtained with the combinations of M_{bio_max} and M_{cap} shown in Table 6.

concentrations of COD. This can be explained by the fact that the higher the maximum concentrations of biomass in a specific point of the granular media, the larger proportion of the accumulated X_{Sf} can be hydrolysed and thus released through the outlet (in the form of S_F, S_A, S_I and S_{NH}) increasing the effluent concentrations of COD and S_{NH}. On the contrary, for M_{cap} = 5 kgVS·m^{-3}, the tendency is different and the effluent concentrations are higher for M_{bio_max} = 0.3 kgVS·m^{-3}, intermediate for M_{bio_max} = 0.1 Kgm^{-3} and the lowest for M_{bio_max} = 0.5 KgVS·m^{-3}. Therefore no clear pattern can be extracted for M_{bio_max} when the values of M_{cap} are relatively small.

Regarding S_{NH} (Fig. 8), for M_{cap} = 15 $kgVS{\cdot}m^{-3}$, the effluent concentrations of this component are almost the same regardless of the value of M_{bio_max}. For the intermediate value of M_{cap} (10 kgVS·m^{-3}), M_{bio_max} = 0.5 kgVS·m^{-3} gives the highest effluent concentration, while for M_{bio_max} = 0.3 kgVSm^{-3} and M_{bio_max} = 0.1 kgVS·m^{-3} the effluent concentrations are almost identical. For the lowest value of M_{cap} (5 kgVS·m^{-3}) there are also differences between the curves, but in this case M_{bio_max} = 0.1 kgVS·m^{-3} gives the lowest effluent concentrations of S_{NH} while M_{bio_max} = 0.5 kgVS·m^{-3} and M_{bio_max} = 0.3 kgVS·m^{-3} give almost the same results.

Therefore, contrarily to what happened for M_{cap}, for M_{bio_max} although some patterns can be detected for the effluent COD concentrations, there is not a clear distinguishable tendency regarding the effluent concentrations of S_{NH} obtained with the different values of this parameter. However, the higher the value of M_{cap}, the larger the difference between the effluent concentrations obtained with the different values of M_{bio_max}.

Therefore, the two model outputs analysed, although in different degrees, are sensitive to changes in the values of M_{cap} and M_{bio_max}. These two parameters represent two different physical processes: M_{bio_max} prevents the limitless growth of bacteria in the pores where substrates concentrations are high, while M_{cap} accounts for the reduction of pore space due to the accumulation of solids that in turn limits the bacterial biomass that can be maintained in the available space. Hence, and as discussed in Samsó and García (2013b) and Samsó and García (2014), each of them individually also has an impact on the distribution and concentration of biomass and accumulated solids in the granular media. For this reason, both parameters are considered essential and the potential benefits of lumping them into a single parameter are not justified.

4. Conclusions

In this work we performed a mesh optimization procedure in order to reduce the simulation time (while maintaining similar numerical accuracy) for subsequent simulations, and we also performed a local sensitivity analysis of parameters M_{cap} and M_{bio_max}.

Results of the mesh optimization procedure indicated that for homogeneous meshes, a positive linear relationship existed between the number of elements and simulated time. The best compromise between numerical accuracy and computational cost was obtained with meshes $M_{0.03}$ and $M_{BIO-PORE}$. Therefore $M_{BIO-PORE}$ was selected as the optimal mesh to carry out the sensitivity analysis.

Despite the range of values given to M_{cap} was smaller than that given to M_{bio_max}, the former parameter proved to be the most sensitive one, and the higher its value the lower the simulated effluent concentrations of COD and S_{NH}. This was due to the fact that for larger values of M_{cap}, more slowly biodegradable solids can accumulate in a specific point, and if there is not enough bacteria to hydrolyse them, they are not released and thus the effluent concentrations of COD and S_{NH} does not increase.

On the other hand, from the values given to M_{bio_max} no clear recognizable pattern on the effluent concentrations of COD and S_{NH} could be observed.

Acknowledgements

Roger Samsó acknowledges the scholarship provided by the Universitat Politècnica de Catalunya (UPC). Authors are also grateful to the European Commission for the financial support of the SWINGS project (Grant Agreement No.: 308502).

References

Batstone, D.J., Keller, J., Angelidaki, I., Kalyuzhny, S.V., Pavlostathis, S.G., Rozzi, A., Sanders, W.T.M., Siegrist, H., Vavilin, V.A., 2002. Anaerobic Digestion Model No. 1 (ADM1). Scientific and Technical Report No 13. IWA Publishing, London, UK.

Brovelli, A., Malaguerra, F., Barry, D., 2009. Bioclogging in porous media: model development and sensitivity to initial conditions. Environ. Model. Softw. 24 (May (5)), 611–626, http://dx.doi.org/10.1016/j.envsoft.2008.10.001.

Cariboni, J., Gatelli, D., Liska, R., Saltelli, A., 2007. The role of sensitivity analysis in ecological modelling. Ecol. Model. 203 (April (1–2)), 167–182, http://dx.doi.org/10.1016/j.ecolmodel.2005.10.045.

Caselles-Osorio, A., Puigagut, J., Segú, E., Vaello, N., Granés, F., García, D., García, J., 2007. Solids accumulation in six full-scale subsurface flow constructed wetlands. Water Res. 41 (March (6)), 1388–1398, http://dx.doi.org/10.1016/j.watres.2006.12.019.

Clement, T.P., Sun, Y., Hooker, B., Peterser, J., 1998. modeling multispecies reactive transport in ground water. Groundw. Monit. Rem. 18 (2), 79–92.

Dimov, I., Georgieva, R., 2010. Monte Carlo algorithms for evaluating sobol sensitivity indices. Math. Comput. Simul. 81 (November (3)), 506–514, http://dx.doi.org/10.1016/j.matcom.2009.09.005.

García, J., Aguirre, P., Mujeriego, R., Huang, Y., Ortiz, L., Bayona, J.M., 2004b. Initial contaminant removal performance factors in horizontal flow reed beds used for treating urban wastewater. Water Res. 38 (April (7)), 1669–1678, http://dx.doi.org/10.1016/j.watres.2004.01.011.

García, J., Chiva, J., Aguirre, P., Alvarez, E., Sierra, J., Mujeriego, R., 2004a. Hydraulic behaviour of horizontal subsurface flow constructed wetlands with different aspect ratio and granular medium size. Ecol. Eng. 23 (November (3)), 177–187, http://dx.doi.org/10.1016/j.ecoleng.2004.09.002.

García, J., Rousseau, D.P.L., Morató, J., Lesage, E., Matamoros, V., Bayona, J.M., 2010. Contaminant removal processes in subsurface-flow constructed wetlands: a review. Crit. Rev. Environ. Sci. Technol. 40 (June (7)), 561–661, http://dx.doi.org/10.1080/10643380802471076.

Hamby, D., 1994. A review of techniques for parameter sensitivity analysis of environmental models. Environ. Model. Asses. 32, 135–154.

Henze, M., Gujer, W., Mino, T., van Loosdrecht, M., 2000. Activated Sludge Models ASM1, ASM2, ASM2d and ASM3.IWA Scientific and Technical Report, 9. IWA Publishing, London, UK.

Langergraber, G., Rousseau, D.P.L., García, J., Mena, J., 2009. CWM1: a general model to describe biokinetic processes in subsurface flow constructed wetlands. Water Sci. Technol. 59 (9), 1687–1697, http://dx.doi.org/10.2166/wst.2009.131.

Mburu, N., Sánchez-Ramos, D., Rousseau, D.P., van Bruggen, J.J., Thumbi, G., Stein, O.R., Hook, P.B., Lens, P.N., 2012. Simulation of carbon nitrogen and sulphur conversion in batch-operated experimental wetland mesocosms. Ecol. Eng. 42 (May), 304–315, http://dx.doi.org/10.1016/j.ecoleng.2012.02.00.

Meyer, D., Chazarenc, F., Claveau-Mallet, D., Dittmer, U., Forquet, N., Molle, P., Morvannou, A., Pálfy, T., Petitjean, A., Rizzo, A., Samsó, R., Scholz, M., Soric, A., Langergraber, G., 2014. Modelling constructed wetlands: scopes and aims – a review. Ecol. Eng. (in press).

Monod, J., 1949. The growth of bacterial cultures. Ann. Rev. Microbiol. 3, 371–394.

Puigagut, J., Villasenor, J., Salas, J., Bécares, E., García, J., 2007. Subsurface-flow constructed wetlands in Spain for the sanitation of small communities: a comparative study. Ecol. Eng. 30 (August (4)), 312–319, http://dx.doi.org/10.1016/j.ecoleng.2007.04.005.

Roache, P.J., 1994. Perspective: a method for uniform reporting of grid refinement studies. J. Fluids Eng. 116, 405–413.

Roy, C.J., 2005. Review of code and solution verification procedures for computational simulation. J. Comput. Phys. 205, 131–156, http://dx.doi.org/10.1016/j.jcp.2004.10.036.

Samsó, R., García, J., 2013a. BIO_PORE, a mathematical model to simulate biofilm growth and water quality improvement in porous media: application and calibration for constructed wetlands. Ecol. Eng. 54, 116–127, http://dx.doi.org/10.1016/j.ecoleng.2013.01.021.

Samsó, R., García, J., 2013b. Bacteria distribution and dynamics in constructed wetlands based on modelling results. Sci. Total Environ. 461–462, 430–440, http://dx.doi.org/10.1016/j.scitotenv.2013.04.073.

Samsó, R., García, J., 2014. The cartridge theory: a description of the functioning of horizontal subsurface flow constructed wetlands for wastewater treatment, based on modelling results. Sci. Total Environ. 473–474, 651–658, http://dx.doi.org/10.1016/j.scitotenv.2013.12.070.

Samsó, R., Meyer, D., García, J., 2014. Subsurface flow constructed wetlands models: review and prospects. In: Vymazal, J. (Ed.), The Role of Natural and Constructed Wetlands in Nutrient Cycling and Retention on the Landscape. Springer, Dordrecht, The Netherlands (in press).

Sin, G., Gernaey, K.V., Neumann, M.B., van Loosdrecht, M.C.M., Gujer, W., 2009. Uncertainty analysis in WWTP model applications: a critical discussion using an example from design. Water Res. 43 (11), 2894–2906, http://dx.doi.org/10.1016/j.watres.2009.03.048.

Sin, G., Gernaey, K.V., Neumann, M.B., van Loosdrecht, M.C.M., Gujer, W., 2011. Global sensitivity analysis in wastewater treatment plant model applications: prioritizing sources of uncertainty. Water Res. 45 (January (2)), 639–651, http://dx.doi.org/10.1016/j.watres.2010.08.025.

Tyroller, L., Rousseau, D.P.L., Santa, S., García, J., 2010. Application of the gas tracer method for measuring oxygen transfer rates in subsurface flow constructed wetlands. Water Res. 44 (July (14)), 4217–4225, http://dx.doi.org/10.1016/j.watres.2010.05.027.